

# Compound winter low wind and cold events impacting the French electricity system: observed evolution and role of large-scale circulation

François Collet<sup>1</sup>, Margot Bador<sup>1</sup>, Julien Boé<sup>1</sup>, Laurent Dubus<sup>2,3</sup>, Bénédicte Jourdier<sup>2</sup>

<sup>1</sup>CECI Université de Toulouse, CERFACS/CNRS, Toulouse, France

<sup>2</sup>RTE, Paris, France

<sup>3</sup>World Energy & Meteorology Council, Norwich, UK

Correspondence to : François Collet ([collet@cerfacs.fr](mailto:collet@cerfacs.fr))

**Abstract.** To reach climate mitigation goals, the share of wind power in the electricity production is set to increase substantially in France. In winter, low wind days are challenging for the electricity system when compounded with cold days that are associated with peak electricity demand. The scope of this study is to characterize the evolution of compound low wind and cold events in winter over the 1950-2022 period in France. Compound events are identified at the daily scale using a bottom-up approach based on two indices relevant to the French energy sector, derived from temperature and wind observations. The frequency of compound events shows high interannual variability, with some winters having no event and others having up to 13. Over the 1950-2022 period, the frequency of compound events has decreased, which is likely due to a decrease in the frequency of cold days. Based on a k-means unsupervised classification technique, four weather types are identified, highlighting the diversity of synoptic situations leading to the occurrence of compound events. The weather type associated with the highest frequency of compound events presents pronounced positive mean sea-level pressure anomalies over Iceland and negative anomalies west of Portugal, limiting the entrance of the westerlies and inducing a north-easterly flow that brings cold air over France and Europe generally. We further show that the atmospheric circulation and its internal variability likely play a role in the observed reduction in cold days, suggesting that this negative trend may not be entirely driven by anthropogenic forcings. However, it is more difficult to conclude on the role of the atmospheric circulation in the observed decrease in compound events.

## 1 Introduction

32 The transition of the energy system, including the reinforced integration of renewable energy, is  
33 necessary to reduce greenhouse gas emissions in accordance with the Paris Agreement. A recent report from  
34 the French electricity transmission system operator (Réseau de Transport d'électricité, 2023 ; hereafter  
35 referred to as RTE) shows that France's energy transition will rely on a widespread electrification of residential  
36 heating, transport, and industry, along with an improvement in energy efficiency (e.g., thermal renovation of  
37 buildings). Therefore, the electricity demand is projected to increase from 475 TWh in 2019 to 580-640 TWh  
38 in 2035, according to scenarios in which France meets its energy transition goals (see scenarios A in RTE,  
39 2023). In light of the future electricity demand, France has expressed its intention to significantly expand its  
40 wind energy capacity in the coming decades. Onshore wind power capacity is planned to increase from 20  
41 GW in 2022 to 30-39 GW by 2035 and substantial additional offshore wind farms are also planned, with a  
42 total projected capacity of 18 GW by 2035 compared to 0.5 GW in 2022 (RTE, 2023).

43 The electricity production and demand can be affected by a range of climate conditions. Regarding  
44 electricity demand during winter, France is known to be one of the most temperature sensitive among  
45 European countries (Bloomfield et al., 2020a). This is mainly explained by the high use of electricity for  
46 residential heating, which is expected to increase over the next decades (RTE, 2023). Hence, cold events will  
47 likely continue to be associated with peak electricity demand based on the projections of the future French  
48 electricity system (RTE, 2023). Besides, part of the electricity production in France relies on renewable  
49 energies that are sensitive to climate conditions including wind speed, solar radiation, and river flows. As the  
50 proportion of renewable energy in the French electricity mix rises, the electricity production will be more  
51 influenced by climate variability. In particular, it is anticipated that a higher proportion of wind power in the  
52 electricity mix may lead to higher risks to the electricity production, especially during low wind events. This  
53 is especially the case in winter when solar generation represents a smaller share of the electricity production  
54 (Grams et al., 2017; Otero et al., 2022b). Hence, in France, it can be challenging to ensure adequate electricity  
55 production and demand due to the occurrence of multivariate compound events (Zscheischler et al., 2020),  
56 such as low wind and cold events, which can create stressful situations. This study aims to characterize  
57 compound low wind and cold events in France.

58 Overall, there is little information in the literature on the observed evolution of compound low wind  
59 and cold events in France and Europe. A body of studies focuses on related events using electricity supply and  
60 production data. For instance, an electricity supply drought is defined by a sequence of days with low  
61 renewable electricity production and high electricity demand (Raynaud et al., 2018). Most of these studies  
62 focus on the characterization of the statistical properties of these events (Otero et al., 2022a, b; Raynaud et al.,  
63 2018; Tedesco et al., 2023) or their drivers (Bloomfield et al., 2020a; Ravestein et al., 2018; Thornton et al.,  
64 2017; van der Wiel et al., 2019a, b). Only a limited number of these studies focus on their temporal evolution  
65 in the context of climate change. Van der Wiel et al. (2019a) show that the frequency of electricity supply  
66 droughts in Europe is reduced in a 2 °C warmer world compared to present day conditions, using projections  
67 from two global climate models. Although there is a gap in the understanding of the past evolution of

68 compound low wind and cold events, changes in low wind or cold events have been investigated  
69 independently. Rapella et al. (2023) showed that the frequency of low wind events has decreased in the ERA5  
70 reanalysis over the 1950-2022 period. However, they focus only on offshore regions such as the Bay of Biscay,  
71 the North Sea, and the Channel, in summer and at the annual scale. Focusing on cold temperature conditions  
72 in winter, the frequency and intensity of cold spells have decreased over the last decades in Europe (Cattiaux  
73 et al., 2010; Seneviratne et al., 2021; Van Oldenborgh et al., 2019). While there is clear evidence that climate  
74 change has led to a reduction in cold events, there are still major uncertainties regarding low wind events. It  
75 is therefore difficult to anticipate how compound low wind and cold events may change in the coming decades  
76 as there is a lack of understanding of their past evolution. An objective of this study is to assess the evolution  
77 of these compound events in the observational record.

78 This work also focuses on the influence of the large-scale atmospheric circulation on the occurrence  
79 and evolution of compound low wind and cold events. The atmospheric circulation is an important driver of  
80 temperature variability (e.g., Plaut and Simonnet, 2001) and wind speed variability (e.g., Najac et al., 2009)  
81 in France, and here we aim to further assess its influence on compound events in winter. In the literature,  
82 different approaches are used to explore the influence of the atmospheric circulation and its variability in  
83 favoring particular meteorological situations that affect the electricity sector. This includes identifying weather  
84 regimes of interest (Otero et al., 2022b; van der Wiel et al., 2019b; Tedesco et al., 2023), targeted circulation  
85 types (Bloomfield et al., 2020b), and circulation regimes based on large-scale conditions leading to critical  
86 situations for the electricity system such as days with extremely high electricity demand (Thornton et al.,  
87 2017).

88 Finally, we investigate to what extent the large-scale atmospheric circulation and its variability  
89 contribute to the past evolution of compound low wind and cold events in France. Several studies found that  
90 recent changes in the large-scale circulation play a role in the winter trend in mean temperature across Europe  
91 (Deser and Phillips, 2023; Sippel et al., 2020; Saffioti et al., 2016), and in the decreasing occurrence and  
92 intensity of cold extremes (Horton et al., 2015; Terray, 2021). Using a dynamical adjustment approach based  
93 on observations (Terray, 2021), we explore the role of the changes in large-scale circulation in the observed  
94 trend in compound low wind and cold events in France.

95 This paper is organized as follows: section 2 presents the data and the method used, section 3 presents  
96 the main results and section 4 includes a conclusion and discussion of the findings.

## 97 **2 Data and Method**

98 In this study, we identify compound low wind and cold events based on a wind capacity factor index  
99 and a temperature index. These indices respectively capture the sensitivity of the French wind power  
100 production to wind speed conditions and the sensitivity of the French electricity demand to temperature  
101 conditions. Thus, compound events as defined in this study correspond to days when the French power system  
102 is challenged by both wind and temperature conditions. In this section, we first introduce the data and

methodology used to define the wind capacity factor and temperature indices. Then, we introduce the methodology used to identify compound low wind and cold events. Finally, the methods used to identify weather types and to assess the role of the large-scale circulation in the evolution of compound events are developed.

## 2.1 Observations and reanalyses of atmospheric variables

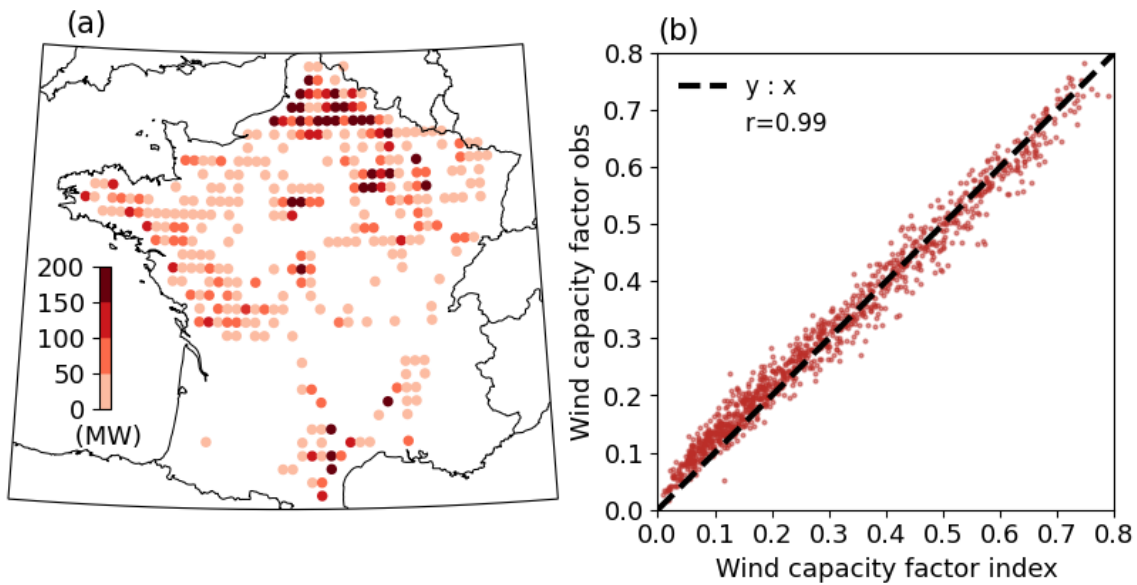
The ERA5 reanalysis data (Hersbach et al., 2020) is used over the period 1950-2022. ERA5 is available on a regular grid with a resolution of about 30 km in Europe. In particular, the hourly wind speed (at 100 m) and the daily near-surface air temperature (at 2 m) are used for the calculation of the wind capacity factor and temperature indices, respectively (section 2.3 and 2.4). Daily mean sea level pressure is also used for the classification of the large-scale circulation into weather types (see section 2.6) and dynamical adjustment (section 2.7). In addition to the ERA5 reanalysis, wind and temperature data from the MERRA-2 reanalysis (Gelaro et al., 2017) are considered. MERRA-2 is available at a horizontal resolution of about 60 km over Europe, over the 1980-2022 period. Hourly near-surface air temperature and wind (at 50 m) are used. We also consider in situ temperature observations from the gridded E-OBS dataset (Cornes et al., 2018) over the 1950-2022 period, available on a regular grid with a horizontal resolution of about 30 km in Europe.

This study is mainly focused on an extended winter period, from November to March, when compound low wind and cold events occur in France. By convention, hereafter, winter 1951 corresponds to the period from November 1950 to February 1951 and so on.

## 2.2 Observations of the wind power production and electricity demand in France

The hourly observed data for the wind power production and electricity demand in France are taken from the `éCO2mix` dataset (<https://odre.opendatasoft.com/explore/dataset/eco2mix-national-cons-def/information/?disjunctive.nature>), over the 2012-2020 period. The French wind power installed capacity is available at 3-monthly time intervals over the 2012-2020 period at <https://www.statistiques.developpement-durable.gouv.fr/publicationweb/549>. The hourly observed wind capacity factor is calculated using the hourly observed wind power production from `éCO2mix`, which is divided by the wind power installed capacity in France of the corresponding 3-monthly interval.

## 2.3 Wind capacity factor index



130

131 Figure 1: (a) Spatial distribution of the wind power installed capacity (MW) in France in 2021 from the  
 132 WindPower.net dataset used for the calculation of the wind capacity factor index. (b) French wind capacity  
 133 factor index as calculated with ERA5 (no unit; X-axis) versus observations (no unit; Y-axis) in winter over the  
 134 2012-2020 period. The correlation coefficient is given in the top left corner, and the black dashed line  
 135 represents the  $y:x$  function.

136

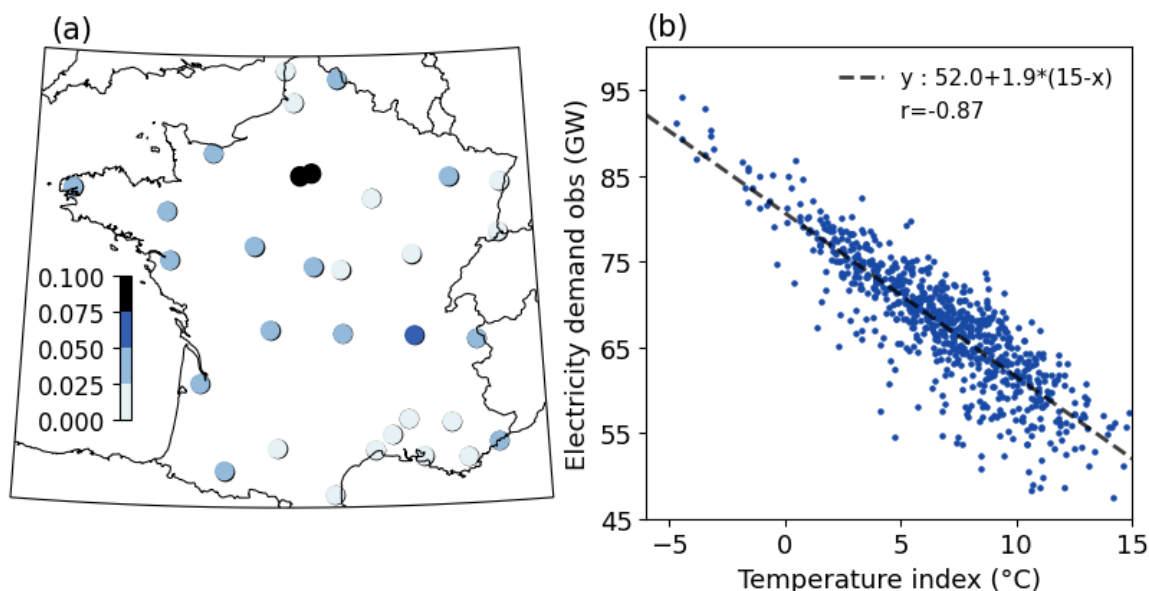
137 Several studies (Bloomfield et al., 2022; Jourdir, 2020; Olauson, 2018; Staffell and Pfenninger, 2016)  
 138 demonstrated that it is possible to calculate hourly wind capacity factor at country-scale with good accuracy  
 139 using wind speed from reanalysis data in Europe. Here, we use a similar approach to calculate the French wind  
 140 capacity factor index over the 1951-2022 period.

141 This approach requires the location, rated power, hub height, and power curves of wind turbines at  
 142 each wind farm site, which are taken from The Wind Power database (<https://www.thewindpower.net/>). Only  
 143 wind farms operational in 2021 are used (i.e., those with “in production” status). This represents a total number  
 144 of 1661 wind farms and a total installed capacity of 19 GW. Wind farms and related wind power installed  
 145 capacity are concentrated in the North-East of France (Figure 1a). While the installed wind power capacity is  
 146 fairly accounted for in this database, there is a substantial amount of missing data regarding the hub heights  
 147 and the power curves (~29 % and ~7 % of wind farms, respectively). Missing data are filled in following the  
 148 methodology introduced in Jourdir (2020), which broadly consists in taking characteristics from wind farms  
 149 identified as similar in terms of rated power, rated diameter, rated wind speed, cut-in and cut-off wind speed.

150 To calculate the wind capacity factor, ERA5 hourly wind speed at 100 m is first interpolated to each  
 151 wind farm site using a nearest neighbor interpolation scheme. The wind speed is then extrapolated at hub  
 152 height using a power law ( $\alpha=0.14$ ; Manwell, 2010; van der Wiel et al., 2019a). Then, using the power curve  
 153 of each wind farm, wind speed at the hub height is converted into power production. Finally, the hourly wind  
 154 capacity factor over France is estimated by summing the power production from all wind farms, and dividing  
 155 this total power production by the total installed capacity. Finally, hourly wind capacity factors are averaged  
 156 to daily values to further identify low wind days (section 2.5).

157 The daily wind capacity factor index computed with this approach is extremely well correlated with  
158 observations over their 9 common winters ( $r=0.99$ , Figure 1b), highlighting the relevance of using ERA5 data  
159 in this context.

## 160 2.4 Temperature index representative of the electricity demand

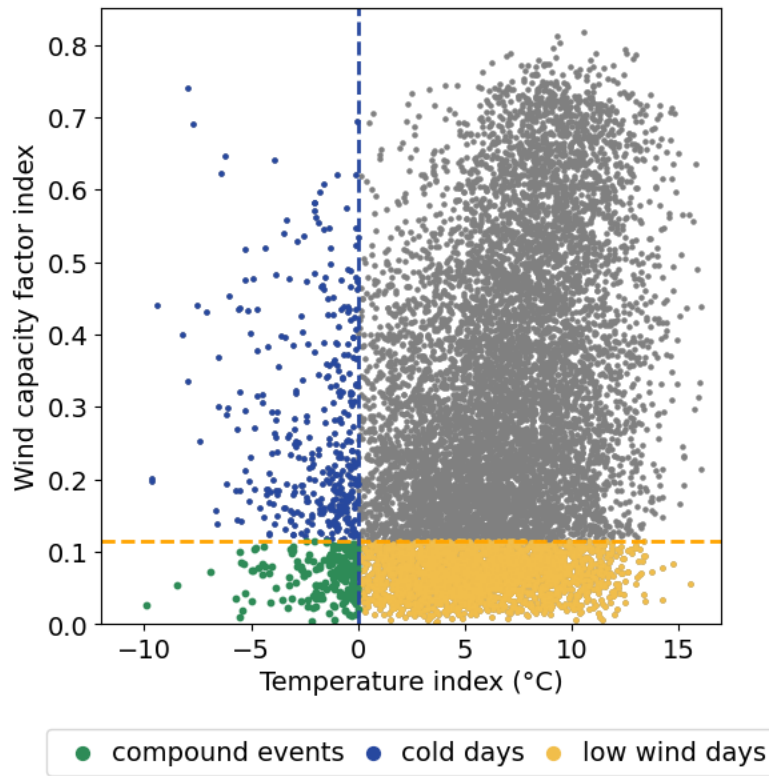


161  
162 Figure 2: (a) Location of the 32 French cities and associated weights (no unit) used for the calculation  
163 of the temperature index. (b) Temperature index as calculated in ERA5 ( $^{\circ}\text{C}$ ; X-axis) versus observations of  
164 the electricity demand (GW; Y-axis) in winter over the 2012-2020 period, excluding week-ends and bank  
165 holidays. The correlation coefficient is given in the top right corner. The linear regression line between the  
166 temperature index and the electricity demand observations is shown by the black dashed line. The  
167 corresponding linear regression equation, in the form  $y = y(15^{\circ}\text{C}) + a \cdot (15^{\circ}\text{C} - x)$ , where  $15^{\circ}\text{C}$  is the threshold  
168 of residential heating and  $a$  the thermosensitivity of the electricity demand, is shown in the top right corner.  
169

170 The temperature index is defined following an approach used operationally by RTE that consists in  
171 calculating a weighted average of temperature data from 32 cities in France (Figure 2a), which is  
172 representative of the electricity demand in France. First, the near-surface air temperature in ERA5 at the grid  
173 cell closest to each city location is selected. Then, the temperature is corrected based on the difference between  
174 the elevation of the grid cell and the elevation of the in situ station for each city, assuming a vertical gradient  
175 of temperature of  $-6.5^{\circ}\text{C}/\text{km}$ . Finally, the weighted average of temperature at the 32 locations is calculated  
176 over the 1950-2022 period.

177 A strong anti-correlation of  $-0.87$  is found between the temperature index and the observed electricity  
178 demand in winter (Figure 2b). This highlights the relevance of the temperature index as a proxy for the French  
179 electricity demand.

## 182 2.5 Identification of low wind days, cold days and associated compound events



183

184 Figure 3: Wind capacity factor index (no units; Y-axis) and temperature index (°C; X-axis) calculated with  
185 ERA5 for each winter day over the 1951-2022 period. Yellow and blue dashed lines show the thresholds used  
186 to identify low wind days and cold days (yellow and blue points, respectively). Compound low wind and cold  
187 events are identified by the green dots.

188 In this study, compound events are defined as days when low wind capacity factor and cold temperature  
189 co-occur (green points in Figure 3). Days of low wind capacity factor (yellow points in Figure 3) are defined  
190 as days with an observed wind capacity factor below 0.15, corresponding to the 23rd percentile of its  
191 distribution in winter. This sample of low wind capacity factor days only captures days with low values of 100  
192 m wind speed over France (see Figure S1). Thus, these events are referred to as low wind days. Cold days are  
193 defined as days with a temperature index below 0 °C, corresponding to the 5th percentile of its distribution in  
194 winter (blue points in Figure 3). In this study, we chose to set a more extreme threshold for the temperature  
195 index compared to the wind capacity factor index because risks to the French power system have historically  
196 been primarily related to the occurrence of cold waves in winter (Añel, 2017). However, depending on future  
197 levels of wind power installed capacity and demand patterns, the sensitivity of the power system to these  
198 thresholds might change. Sensitivity tests exploring different thresholds for both indices are therefore included  
199 in Supplementary Materials. These tests show limited sensitivity to thresholds for the definition of compound  
200 events, except for the long-term trend in the observed occurrence of compound events over the 1951-2022  
201 period.

## 202 2.6 Weather types of low wind days

203 A classification of mean sea-level pressure fields on low wind days (i.e., low wind capacity factor day)  
204 is conducted using the k-means unsupervised classification method (e.g., Cassou, 2008; Falkena et al., 2020).

205 This allows classifying daily synoptic conditions into different large-scale atmospheric circulation types, or  
206 weather types. Here, low wind days solely are considered for the classification instead of compound low wind  
207 and cold events because the corresponding sample size is larger (2549 days compared to 182 days,  
208 respectively; see Figure 3, Figure 4b, and further discussions in section 3). In other words, the weather types  
209 represent clusters of low wind days with similar large-scale circulation patterns. In a second phase, we examine  
210 how cold days are distributed across these different weather types. Finally, we can thus assess the number of  
211 compound events for each identified weather type.

212 This classification algorithm is first applied repeatedly for different domains and cluster numbers. The  
213 objective is to minimize locally the ratio of intra-type to inter-type variance of the temperature index, while  
214 keeping a reasonable number of weather types. Thanks to this procedure, the classification of low wind days  
215 that allows for the best differentiation of the temperature index is chosen. This procedure leads to a domain  
216 whose limits are [30 °W-30 °E/33°S-70°N], which covers the North-Western Europe region, and a total  
217 number of four clusters.

## 218 **2.7 Dynamical adjustment**

219 The main objective of dynamical adjustment is to derive an estimate of the contribution of large-scale  
220 atmospheric circulation to the variations of a variable of interest (Terray, 2021; Deser et al., 2016; Sippel et  
221 al., 2019). In this study, we use dynamical adjustment to estimate the contribution of large-scale circulation  
222 to the variations of cold days, low wind days, and compound events.

223 First, we estimate the contribution of large-scale circulation to the wind capacity factor and  
224 temperature indices, hereafter referred to as their dynamic component. To that purpose, the constructed  
225 analogue approach is used (Terray, 2021; Boé et al., 2023; Deser et al., 2016). Following Lorenz (1969),  
226 analogues are defined as days with very similar large-scale circulation. As finding genuinely good analogues  
227 in a finite database could be difficult, synthetic analogues can be constructed through the linear combination  
228 of the large-scale circulation corresponding to a large number of more or less good analogues (Van Den Dool,  
229 1994).

230 First, for each target day of the winters 1951-2022, the 400 closest analogues are searched in winter  
231 using the Euclidean distance calculated with ERA5 mean sea-level pressure interpolated on a  $2^\circ \times 2^\circ$  grid on  
232 the North-Western Europe domain (section 2.6). The winter of the target day is excluded from the search pool.  
233 Then for each target day, a subset of 200 analogues is randomly selected from the 400 analogues, and the  
234 optimal linear combination of this subset of 200 analogues that best matches the mean seal level pressure of  
235 the target day is calculated. This allows obtaining a constructed analogue for the target day. This procedure is  
236 repeated 200 times, to obtain 200 constructed analogues for each target day and the corresponding 200 sets of  
237 optimal weights. While the 200 constructed analogues of each target day have very similar large-scale  
238 circulation to the target day, this procedure, together with the large number of analogues used allows us to



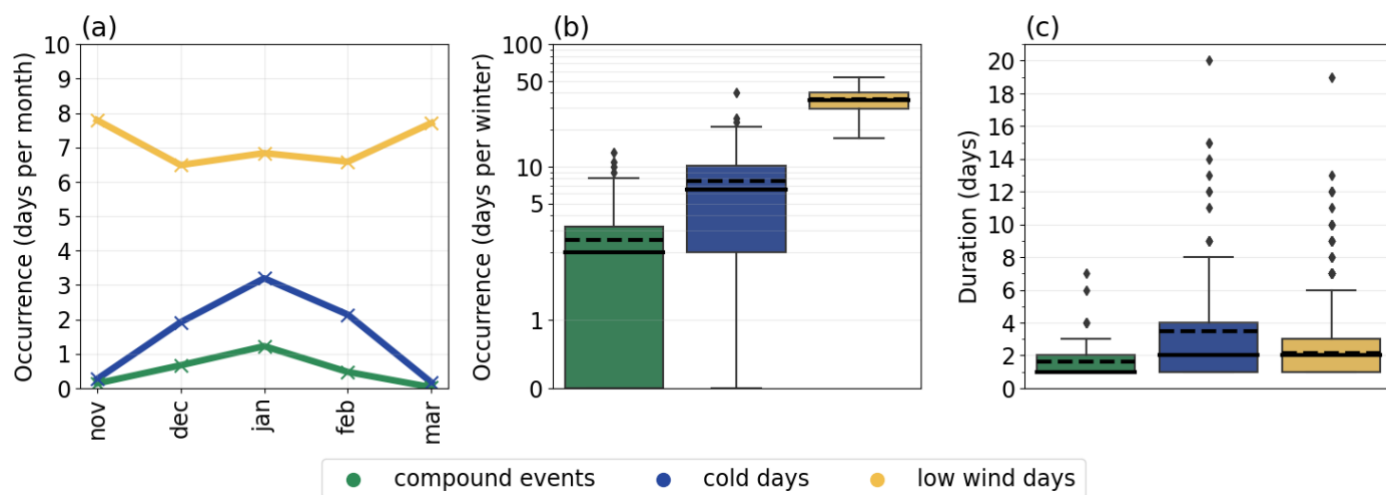
239 sample different land surface and ocean conditions that might otherwise influence the estimate of the dynamic  
240 components (Terray, 2021).

241 For each target day, the wind capacity factor and the temperature indices are then reconstructed by  
242 applying the same set of optimal linear weights to the corresponding wind capacity factor index and detrended  
243 anomalies of the temperature index, respectively. There are 200 reconstructions of the wind capacity factor  
244 and the temperature index per day over the winters 1951-2022. As we are interested in separating the trend  
245 due to large-scale circulation from thermodynamically-forced changes, an estimate of the forced trend of the  
246 temperature index anomaly for each winter month is removed before applying the dynamical adjustment. This  
247 low-frequency trend is estimated using a low-frequency LOESS smoother as done in Terray (2021). Finally,  
248 a best estimate of the dynamic component of the wind capacity factor index and the temperature index are  
249 derived by averaging the 200 reconstructions of the wind capacity factor index and the temperature index,  
250 respectively.

251 To isolate the impact of large-scale circulation on the evolution of compound events, we define  
252 circulation-induced compound events. These are virtual events based only on the contribution of large-scale  
253 circulation. First, circulation-induced low wind days and cold days are identified using the same thresholds as  
254 for the definition of low wind days and cold days (i.e., the 5th percentile and the 23rd percentile of the extended  
255 winter distribution, respectively; Section 2.5), but this time on the dynamic component of the wind capacity  
256 factor and temperature indices, respectively. Finally, circulation-induced compound events are identified as  
257 days when both the circulation-induced low wind days and circulation-induced cold days virtually occur.

### 258 3. Results

#### 259 3.1 Climatological characteristics and observed evolution of compound low wind and cold events



260

261 Figure 4: (a) Monthly mean number of compound low wind and cold events (green), cold days (blue), and low  
262 wind days (yellow); Distributions of (b) the number of days per winter and (c) duration of compound low  
263 wind and cold events, cold days, and low wind days in winter over the 1951-2022 period in ERA5. The solid  
264 line and the dashed line in the boxplots in (b) and (c) show the median and the average, respectively.

265

266

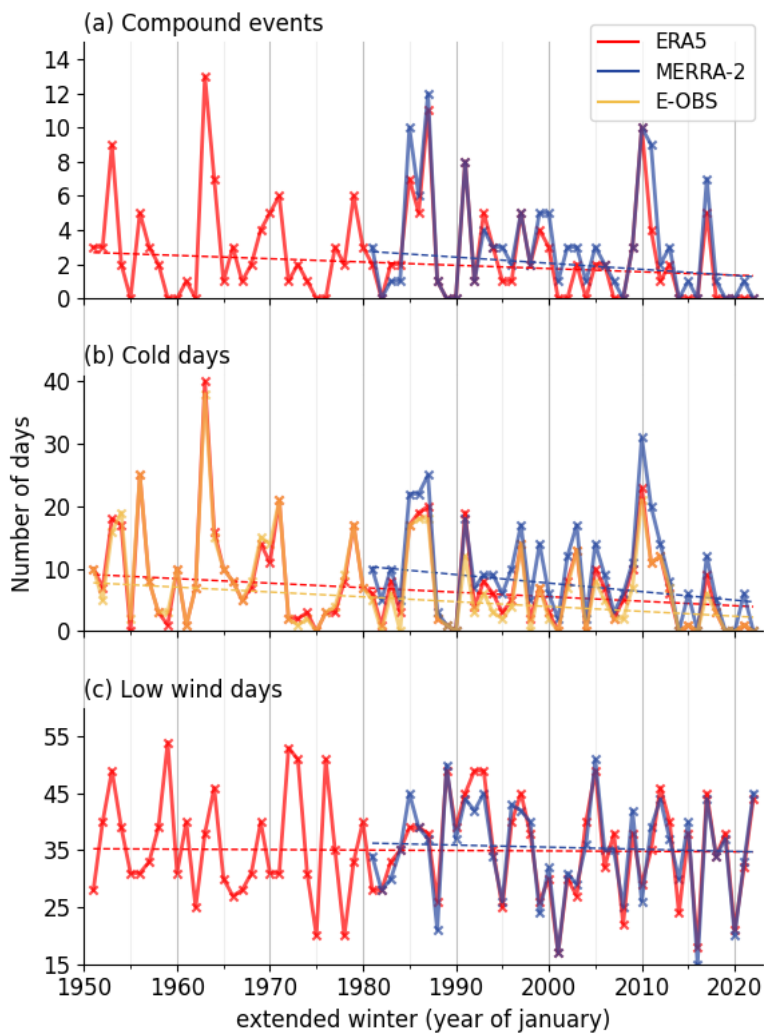
During the extended winter period (November to March), there are clear monthly variations in the occurrence of compound events, which are concentrated in mid-winter months (i.e., December to February) and peak in January (Figure 4a). This is well explained by cold days that have similar monthly variations, while low wind days (i.e., days with low wind capacity factor) predominantly occur during early and late winter months (i.e., November and March).

271

The median number of compound events per winter (2 days; Figure 4b) is a third of the median number of cold days per winter (6 days; Figure 4b). The median number of low wind days per winter reaches 35 days and is therefore substantially higher than for compound events and cold days. In terms of year-to-year variability, we find that the number of compound events ranges from 0 to 13 days per winter, while there are from 0 to 40 cold days and 17 to 54 low wind days. When compared to the mean, the interannual variability is thus higher for the occurrence of compound events and cold days compared to low wind days.

277

On average in winter, the duration of compound events is estimated to be around 2 consecutive days, 3 days for cold days, and 2 days for low wind days (Figure 4c). The maximum duration of compound events is 7 consecutive days, corresponding to the period between 17 and 23 January 1987, at the end of a severe 13-day cold spell. Overall, compound low wind and cold events are relatively rare and generally short-lived, but they can last for a few days and up to a week occasionally.



282

283 Figure 5: Interannual evolution of the number of (a) compound low wind and cold events, (b) cold days, (c)  
 284 and low wind days per winter in ERA5 (in red; 1951-2022), MERRA-2 (in blue; 1981-2022) and E-OBS (in  
 285 yellow; 1951-2022) datasets. Dashed lines show the linear trend (calculated with the Theil-Sen estimator; see  
 286 Table 1 for the slope value and associated significance).

287

Data	ERA5		MERRA-2		E-OBS	
	1951-2022	1981-2022	1951-2022	1981-2022	1951-2022	1981-2022
Compound events	<b>-0.19 (0.02)</b>	<b>-0.43 (0.01)</b>	/	-0.36 (0.1)	/	/
Cold days	<b>-0.72 (0.02)</b>	-1.03 (0.08)	/	-1.36 (0.08)	<b>-0.78 (0.0)</b>	-0.67 (0.16)
Low wind days	-0.08 (0.59)	-0.45 (0.48)	/	-0.37 (0.72)	/	/

288 Table 1: Trend (slope in days/decade) and associated p-value, in the number of compound low wind and cold  
 289 events, cold days, and low wind days in ERA5, MERRA-2 and E-OBS over their respective time period (as  
 290 indicated in the first row). The slope is calculated with Theil-Sen estimator and the p-value with the Mann-  
 291 Kendall test. Significant trends with  $p < 0.05$  are shown in bold. Cells with « / » correspond to missing data.

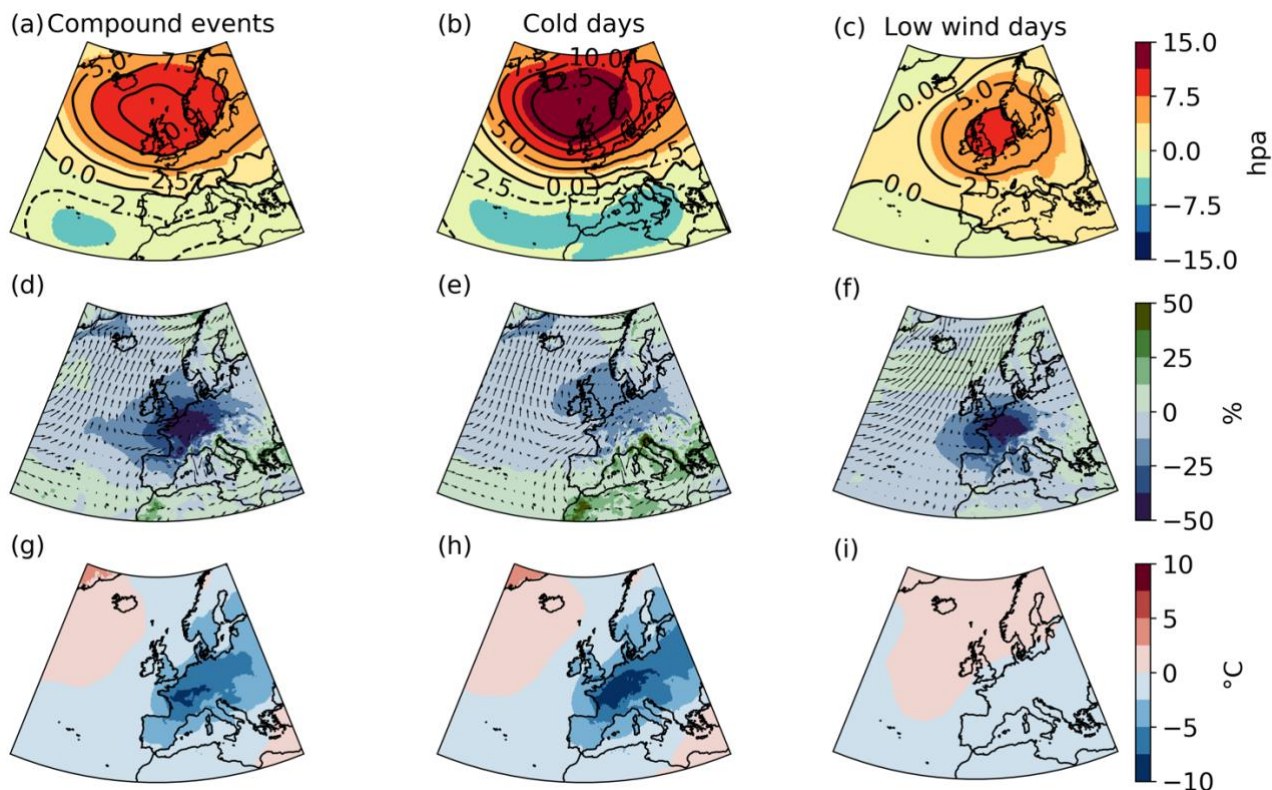
292 Further looking into the year-to-year differences in the number of compound low wind and cold events,  
 293 we find substantial interannual variability (Figure 5a). Some winters stand out as extreme cases, such as 1963,  
 294 1985, 1987, and 2010. In particular, the exceptional winter 1963, is the most extreme winter with 13 days of  
 295 compound events (Figure 5b). Winter 1963 is the coldest winter ever recorded over Western Europe (Hirschi  
 296 and Sinha, 2007) and our results further show that low wind days were co-occurring with some of these cold  
 297 days. Overall, there is a good agreement between ERA5 and MERRA-2 over the shorter 1981-2022 period.  
 298 This includes the characterization of the most extreme winters in terms of compound events, although  
 299 MERRA-2 generally shows a slightly higher number of compound events per winter.

300 The interannual variability of compound events is primarily driven by the variability of cold days  
 301 compared to the variability of low wind days ( $r=0.86$  and  $r=0.19$  in ERA5, respectively; Figure 5a,b). In  
 302 particular, the highest numbers of compound events are found in years also characterized by the highest  
 303 numbers of cold days, but not necessarily in years with the highest numbers of low wind days (e.g., 1963,  
 304 1987, 2010, Figure 5a,b,c). This is due to the more extreme threshold applied on the temperature index and  
 305 therefore the larger sample of low wind days per winter on average compared to the number of cold days  
 306 (section 2.5 and sensitivity analyses in the Supplementary Material).

307 Over the 1951-2022 period, there is a significant decrease in the number of compound events per winter  
 308 in ERA5 (-0.19 day per decade; Figure 5a and Table 1). Over the shorter period in common between ERA5  
 309 and MERRA-2, compound events have also decreased significantly in ERA5, and at a higher rate (-0.43 day  
 310 per decade). MERRA-2 shows a slightly weaker decrease in compound events (-0.36 day per decade)  
 311 compared to ERA5, which is not significant at the 0.05 level ( $p=0.10$ ). In terms of low wind days, no trend is  
 312 detected in ERA5 over both the longer and shorter periods, and both reanalyses agree on the absence of a  
 313 trend. Conversely, cold days have significantly decreased over the longer period in both the ERA5 reanalysis  
 314 and the E-OBS observations, and at a similar rate of -0.72 and -0.78 day per decade (respectively; Figure 5b  
 315 and Table 1). Interestingly, over the shorter period in common with ERA5, MERRA-2, and E-OBS, the

316 significance of the negative trend is lost, suggesting that this period might be too short for the influence of  
317 anthropogenic forcings to emerge from internal variability, contrary to what is observed on the longer period.

### 318 3.2 Role of large-scale circulation



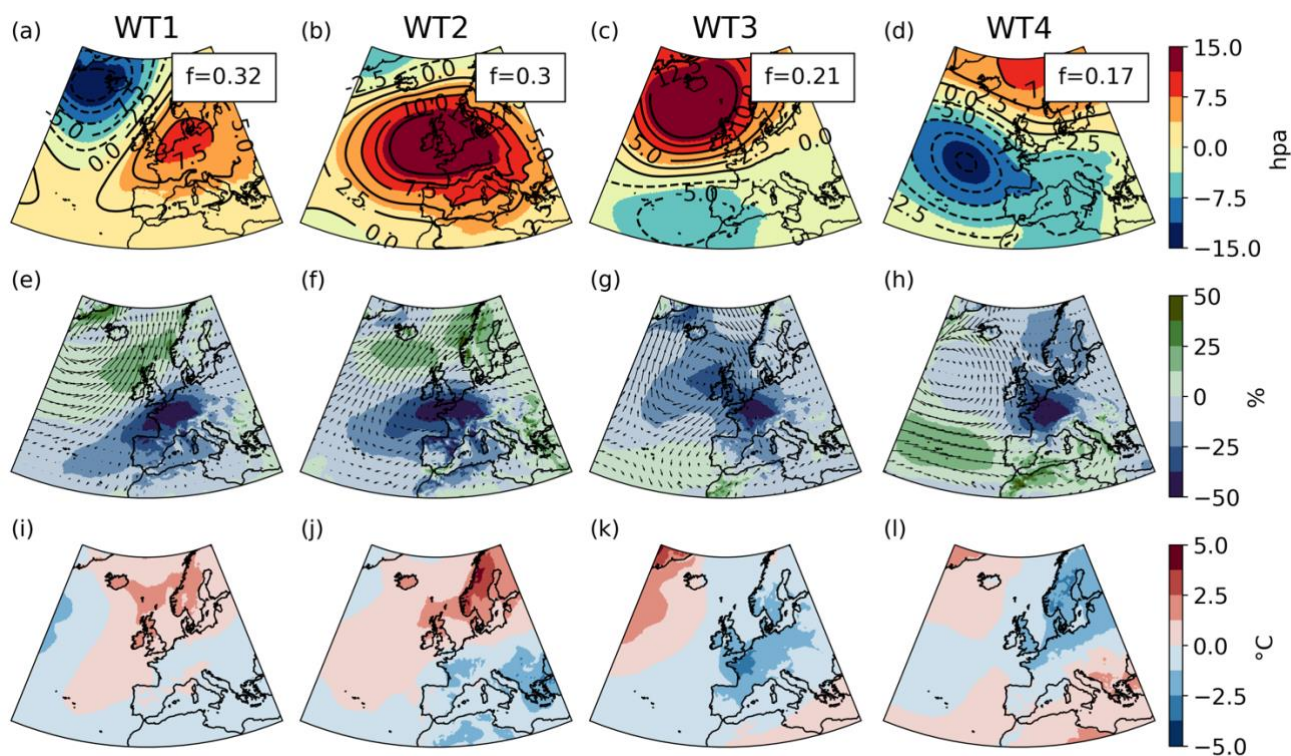
319  
320 Figure 6: Composite of (a,b,c) mean sea-level pressure anomalies (hPa) with solid and dashed  
321 contours corresponding to positive and negative anomalies respectively, (d,e,f) 100 m wind speed relative  
322 anomalies (% of climatological mean; shadings) and wind direction (arrow), and (g,h,i) near-surface air  
323 temperature anomalies, in average during (a,d,g) compound low wind and cold events, (b,e,h) cold days, and  
324 (c,f,i) low wind days. Relative anomalies for both the temperature and 100 m wind speed are calculated with  
325 respect to their daily climatology (1950-2022) in ERA5 (smoothed with a 15-day moving average).

326 On average, the synoptic conditions leading to the occurrence of compound low wind and cold events  
327 (i.e., compound low wind capacity factor and cold events) are characterized by strong positive mean sea-level  
328 pressure anomalies over the British Isles and relatively less intense negative anomalies centred on the Azores  
329 (Figure 6a). Overall, the average large-scale circulation during compound events is very well spatially  
330 correlated with that of cold days (Figure 6b), but the intensity of the positive anomalies and associated pressure  
331 dipole are weaker in the case of compound events. The anomalies in mean sea-level pressure are somehow  
332 different during low wind days compared to compound and cold events. Positive sea level pressure anomalies  
333 are found further south over the North Sea, with relatively lower intensity, and the negative anomalies over  
334 the Azores are not as clear (Figure 6c).

335 On average during the compound events defined for the French electricity system solely, negative  
336 anomalies of wind speed and temperature expand over a wider European domain, comprising Germany and  
337 the British Isles, with anomalies up to -40 % and -7.5 °C, respectively (Figure 6d, g). The negative temperature

338 anomalies over France and surrounding countries are slightly weaker during compound events compared to  
 339 cold days (Figure 6g,h). These cold anomalies are induced by a north-easterly flow advecting cold polar air  
 340 towards western Europe. During cold days, and compared to compound events, the negative anomalies in  
 341 wind speed are less intense, the advection of cold air is stronger, and thus colder temperatures are experienced  
 342 over western Europe. During low wind days, negative wind anomalies are found over western Europe, with  
 343 intensities rather similar to those during compound events, along with neutral temperature anomalies (Figure  
 344 6f,i). We find relatively higher similarities in the mean sea-level pressure anomalies between cold days and  
 345 compound events compared to between low wind days and compound events. This can be explained by a more  
 346 extreme threshold used for cold days compared to low wind days in the definition of compound events. Note  
 347 that the sensitivity to thresholds used in the definition of compound events is documented in Supplementary  
 348 Materials. While we find that sea-level pressure anomalies between low wind days and compound events  
 349 compare better when setting a more extreme threshold for low wind days in the compound event definition,  
 350 the main conclusions of this work are generally not sensitive to these thresholds (Figure S3). It is important to  
 351 acknowledge that these average climate conditions might hide a variety of different large-scale atmospheric  
 352 circulations, further explored in the following section using a weather type analysis.

353



354

355

356 Figure 7: Composite of (a,b,c,d) sea-level pressure anomalies (hPa) with solid and dashed contours  
 357 corresponding to positive and negative anomalies respectively, (e,f,g,h) 100 m wind speed relative anomalies  
 358 magnitude (% of climatological mean; shadings) and wind direction (arrows), and (i,j,k,l) near-surface air  
 359 temperature anomalies corresponding to the weather types of low wind days (a,e,i) WT1, (b,f,j) WT2, (c,g,k)  
 360 WT3 and (d,h,l) WT4. The frequency (f) of the weather types is shown in the upper right corner in panels  
 361 a,b,c,d.

362

363 Four weather types are obtained by classifying the mean sea-level pressure during low wind days using  
364 the k-means algorithm (see section 2.6). We then assess the distribution of compound low wind and cold  
365 events across these four weather types to identify the most favorable synoptic situations leading to the  
366 occurrence of these compound events in France, and over western Europe more generally.

367 The frequency of weather types of low wind days is rather similar, and ranges from 0.17 (WT4) to 0.32  
368 (WT1). While all four weather types are characterized by low wind conditions (by definition), interestingly,  
369 they are also associated with cold temperatures in France and they reveal a diversity of large-scale atmospheric  
370 conditions (Figure 7):

- 371 • WT1 is characterized by positive mean sea-level pressure anomalies over the Netherlands and  
372 northern Germany, and negative anomalies over Iceland. The positive anomalies block the entry  
373 of the westerlies at the western border of Europe and deviate them further north, thus advecting  
374 relatively warm and humid air over northern Europe, and inducing a substantial decrease in wind  
375 speed along with cold anomalies in France and western Europe.
- 376 • WT2 shares blocking-like characteristics with WT1, but with more intense positive mean sea level  
377 pressure anomalies and over a wider domain extending further west, pushing the negative mean  
378 sea-level pressure anomalies further to the north-western corner of the domain. As in WT1, the  
379 westerlies are derived north of Europe, inducing a similar dipole of warmer temperatures in the  
380 north and colder temperatures under the positive pressure anomalies. In France and southern  
381 Europe in general, and compared to WT1, the negative anomalies in wind and temperature are  
382 enhanced because of the amplified positive pressure anomalies.
- 383 • WT3 shows pronounced positive mean sea-level pressure anomalies over Iceland and negative  
384 anomalies west of Portugal. This WT resembles the most to the average atmospheric conditions  
385 during compound events (Figure 6a). The dipole of pressure anomalies results in a strong north-to  
386 north-easterly flow advecting cold air masses from Scandinavia to France. This weather type is  
387 associated with the coldest temperatures over France compared to the other weather types, and  
388 generally over the entire European domain that also experiences low wind conditions.
- 389 • WT4 is rather different from WT1, WT2 and WT3 as it is characterized by substantial negative  
390 mean sea-level pressure anomalies in the eastern Atlantic and positive anomalies over the  
391 Norwegian Sea. These pressure anomalies induce low wind conditions in France and generally the  
392 northern part of Europe, and a reinforcement of the westerlies in the southern part of the domain.  
393 This is associated with colder temperatures in the north, including the northern part of France, and  
394 positive or low temperature anomalies in south-western Europe.

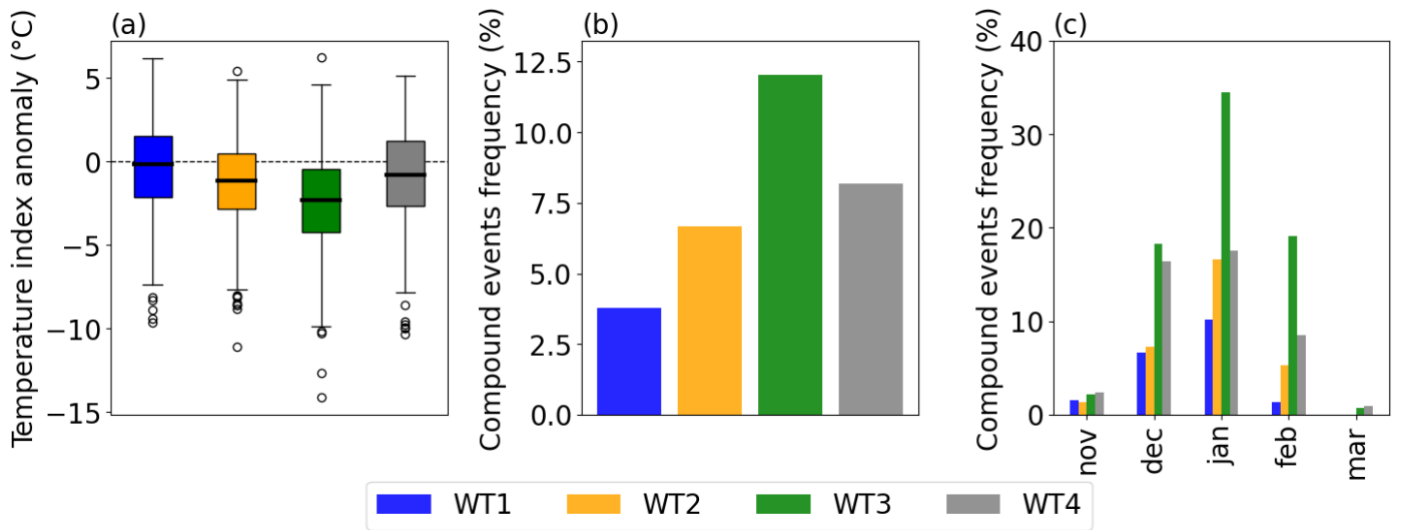


Figure 8: (a) Distribution of temperature index anomalies for each weather type of low wind days (WT; as defined in Figure 7 and indicated in inserted legend); (b) Frequency of compound low wind and cold events for each weather type of low wind days (in % of the weather type size). (c) Frequency of compound low wind and cold events for each weather type of low wind days and each individual winter month (in % of the weather type size for a given month). Temperature index anomalies are calculated with respect to the daily climatology (1950-2022) in ERA5 (smoothed with a 15-day moving average).

The temperature index shows a substantial variability within each weather type of low wind days (Figure 8a). All weather types present very cold days, with anomalies as large as  $-10\text{ }^{\circ}\text{C}$  for WT1 and WT4, and  $-14\text{ }^{\circ}\text{C}$  for WT3. WT3 is the coldest weather type and WT1 is relatively warmer than the others over France. The frequency of compound events when a particular weather type occurs varies from 4 % in WT1 to 12 % in WT3, while WT2 and WT4 present similar values of 7 % and 8 % (Figure 8b). Importantly, the weather type WT3, which is associated with the highest frequency of compound events, also leads to negative anomalies in wind speed and temperature across the majority of Europe (Figure 7c,g,k). This suggests that this weather type might challenge the electricity system on the larger scale of western Europe.

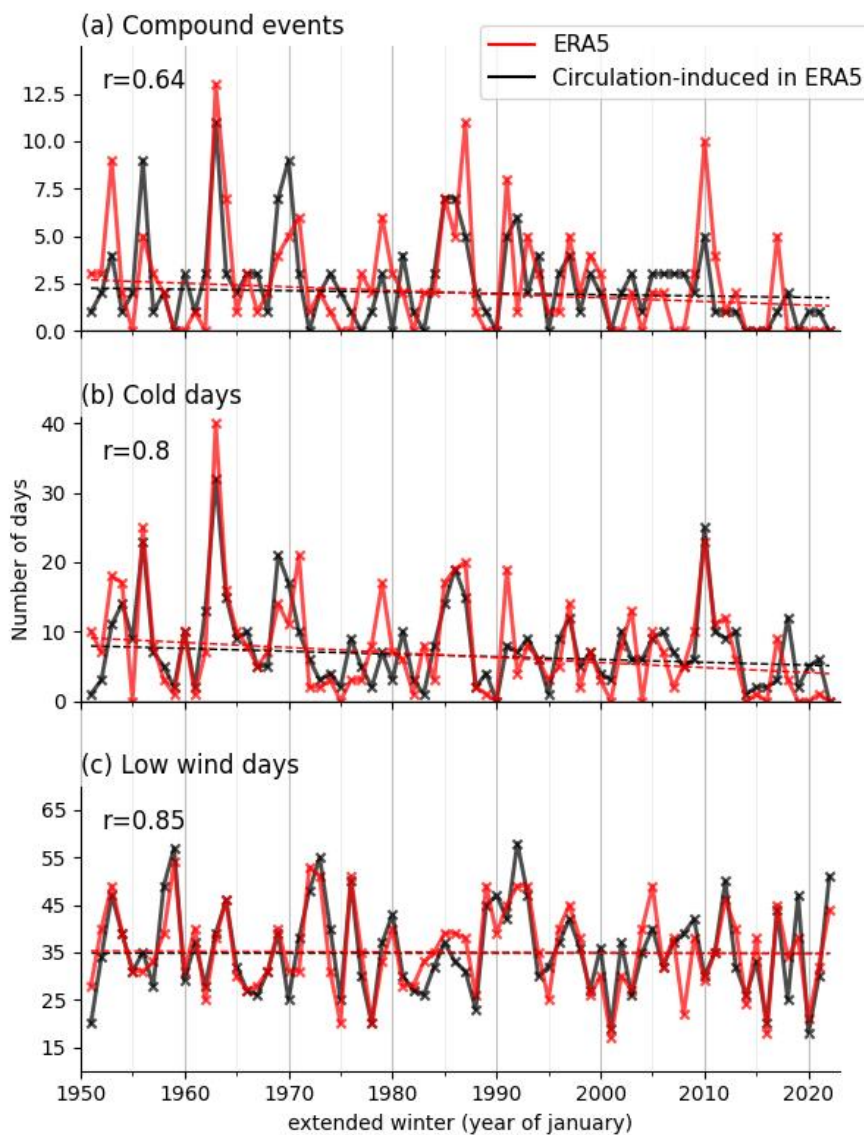
The frequency of compound events in each weather type shows important monthly variations. For all weather types, the frequency of compound events is higher in January, when the climatological temperature reaches its lowest values, compared to other months (Figure 8c). This is especially the case for WT3, for which nearly 35 % of days occurring in January are compound events. This important role of the temperature seasonality within each weather type is consistent with the overall seasonality of compound events discussed in section 3.1.

WT1	WT2	WT3	WT4
0.0 (0.78)	0.56 (0.16)	-0.27 (0.29)	<b>-0.59 (0.01)</b>

Table 2: Trend (slope in days/decade) and associated p-value in the frequency of each weather type of low wind days (WT; as defined in Figure 7) in winter over the 1951-2022 period in ERA5. The slope is calculated with the Theil-Sen estimator and the p-value is calculated with the Mann-Kendall test. Significant trends with  $p < 0.05$  are shown in bold.

424 Only the frequency of WT4 shows a significant negative trend over the 1951-2022 period (-0.59 day per  
 425 decade,  $p=0.01$ ; Table 2). The frequency of WT2 is found to increase (+0.56 day per decade), whereas WT3,  
 426 which is associated with the highest frequency of compound events, decreases (-0.27 day per decade) over the  
 427 observed period. These trends for both WT2 and WT3 are however not significant.

428 To estimate the contribution of the trends in weather type frequencies on the overall evolution of  
 429 compound events, trend values are multiplied by the frequency of compound events for each corresponding  
 430 weather type, as done in Horton et al. (2015). Then, the respective contributions from all four weather types  
 431 are added to estimate the overall influence of the trends in weather type frequencies. This leads to a weak  
 432 decrease in the frequency of compound events of 20 %. This analysis suggests a relatively minor influence of  
 433 large-scale circulation on the trend of compound events. However, due to significant intra-type variability, a  
 434 change in the frequency of a few weather types may not capture the full range of circulation changes.  
 435



436  
 437 Figure 9: Interannual evolution of the number of (a) circulation-induced compound low wind and cold events,  
 438 (b) cold days, and (c) low wind days in winter over the 1951-2022 period in ERA5. For each event, the value  
 439 of the correlation coefficient between the inter-annual evolution and its respective circulation-induced  
 440 evolution is shown in the upper left. Dashed lines show the linear trend (calculated using the Theil-Sen  
 441 estimator; see Table 3 for the slope value and associated p-value).



	Compound events	Cold days	Low wind days
ERA5	<b>-0.19 (0.02)</b>	<b>-0.72 (0.02)</b>	-0.08 (0.59)
Circulation-induced in ERA5	<b>-0.14 (0.04)</b>	-0.40 (0.14)	-0.21 (0.75)

444 Table 3: (first row) Trend (slope in days/decade, and associated p-value) in the frequency of low wind days,  
 445 cold days, and compound low wind and cold events in winter over the period 1951-2022 in ERA5 (first row;  
 446 same trend estimates as in Table 1) and in their respective circulation-induced events (second row; section  
 447 2.7). The slope is calculated with the Theil-Sen estimator and the p-value is calculated with the Mann-Kendall  
 448 test. Significant trends with  $p < 0.05$  are shown in bold.

449 The dynamical adjustment approach described in section 2.7 is now used to better quantify the role of  
 450 the atmospheric large-scale circulation in the evolution of compound low wind and cold events. The  
 451 interannual variability in the occurrence of both cold days and low wind days is very well explained by the  
 452 large-scale circulation (correlations with the corresponding circulation-induced event of 0.80 and 0.85,  
 453 respectively; Figure 9a,b). Therefore, the interannual variability in the number of compound events is also  
 454 well explained by the large-scale circulation (correlations with the circulation-induced compound events of  
 455  $r=0.64$ , Figure 9a). Extreme winters in terms of compound events such as 1963, 1987, or 2010 are due to a  
 456 large extent to the large-scale circulation. Interestingly, circulation-induced cold days substantially decrease  
 457 (-0.40 day per decade; Table 3), although the p-value does not reach the 0.05 significance level ( $p\text{-value}=0.14$ ).  
 458 Large-scale circulation may therefore have contributed to more than 50 % of the decline in cold days  
 459 occurrence (-0.72 day per decade, Table 3) observed between 1951 and 2022, suggesting that anthropogenic  
 460 forcing may not be the only driver of this trend. Similarly, circulation-induced compound events show a  
 461 decrease (-0.14 day per decade, Table 3) over the 1951-2022 period ( $p\text{-value}=0.04$ ). However, both the trend  
 462 significance and the magnitude of the slope are sensitive to the parameters used in the dynamical adjustment  
 463 (not shown). Thus, the robustness is too weak to draw conclusions on the role of the large-scale circulation on  
 464 the decrease in compound events. Finally, there is no significant trend in the circulation-induced low wind  
 465 days.

#### 466 4. Discussion and conclusions

467 In the context of the energy transition, compound low wind capacity factor and cold events could  
 468 present a stronger threat to the adequacy between the electricity production and demand in France. Therefore,  
 469 it is crucial to characterize these climate compound events and to better understand how their frequency has  
 470 changed in the past to better anticipate how they could evolve in the coming decades.

472 Compound events are defined with ERA5 data over the 1950-2022 period using a wind capacity factor  
 473 index, and a temperature index that captures the current sensitivity of the electricity demand in France to

474 temperature. As compound events mainly occur between November and March, our analyses focus on this  
475 period.

476  
477 Compound events are quite rare (2 days per winter on average), with a peak occurrence in January.  
478 They are generally short-lived, with a mean duration of 2 consecutive days although they can last up to 7  
479 consecutive days. There are large interannual differences in the number of compound events, from 0 to 13  
480 days per winter.

481 Over the observational record, we find a statistically significant decrease in compound events  
482 frequency (-0.19 day per decade) that tends to have amplified over the last four decades. This decrease is likely  
483 driven by the significant negative trend in cold days, while the frequency of low wind days shows no  
484 significant trend. Overall, these results suggest a decrease in climate-related risks to the adequacy between  
485 electricity demand and supply related to compound events over the observed period, considering the current  
486 electricity system.

487 The role of the large-scale atmospheric circulation in the occurrence of compound events is assessed  
488 using a set of four weather types derived from the unsupervised k-means classification technique applied to  
489 low wind days. The frequency of compound events in each weather type ranges from 4 % to 12 %. This reveals  
490 a diversity of large-scale atmospheric circulations that can lead to the occurrence of compound events in  
491 France. The weather type associated with the highest compound events frequency (WT3) presents pronounced  
492 positive sea-level pressure anomalies over Iceland and negative anomalies west of Portugal. This weather type  
493 leads to negative anomalies of wind speed and temperature throughout Europe, which might pose challenges  
494 to the electricity system on a larger scale than just in France. Other studies focusing on compound low wind  
495 and cold events at the scale of Europe also highlight the role of large-scale circulation in compound event  
496 occurrence. Bloomfield (2019) and Tedesco (2023) find that pronounced positive mean sea-level pressure  
497 anomalies over Northern Europe and negative anomalies over the Azores lead to a large number of compound  
498 events in Central and Western Europe, and this circulation pattern projects well onto the weather type WT3 of  
499 this study. Similarly, Otero (2022) finds that a particular weather type (called Greenland blocking), which is  
500 similar to our weather type WT3, increases the probability of compound events in Europe. This is also true  
501 for a second weather type (called European blocking) that projects relatively well onto our weather type WT2.  
502 Hence, in this study, we identify large-scale circulation patterns associated with compound events in France  
503 that compare broadly with previous findings focused over Europe. There are slight discrepancies in the  
504 location of the positive and/or negative anomalies, and these might be partly explained by differences in the  
505 particular domain of interest. Other methodological differences such as weather types calculation or definition  
506 of compound events might also explain some differences.

507 Overall, we find that the large-scale atmospheric circulation contributes substantially to the occurrence  
508 of compound events and explains an important part of their interannual variability. Interestingly, the large-  
509 scale atmospheric circulation shows a contribution of approximately 50 % of the observed decrease in cold

510 days over the 1951-2022 period in ERA5. Similarly, Deser and Phillips (2023) found that large-scale  
511 circulation contributes to a third of the mean winter temperature trend in Europe over the last decades.  
512 Assuming that observed changes in the large-scale circulation are mainly driven by internal climate variability  
513 (Shepherd, 2014), these results suggest that, over the last few decades, climate variability likely reinforced the  
514 long-term decline in cold events in response to warming. This may not continue in the near future, potentially  
515 leading to a temporary increase in the occurrence of cold events. Finally, we cannot conclude on the role of  
516 large-scale circulation in the decrease of compound events as our methodology exhibits sensitivity to its  
517 parameters.

518  
519 In this study, compound low wind capacity factor and cold events are identified using a straightforward  
520 approach that consists of identifying cold days and low wind capacity factor days independently. This has the  
521 advantage of allowing the assessment of the relative contribution of cold days and low wind capacity factor  
522 days to the decrease in compound events. Another approach consists in identifying compound events as days  
523 with high residual load (i.e., electricity demand minus wind power production), i.e., days that need important  
524 availability of other power sources than wind power, such as hydro-electricity or nuclear generation  
525 (Bloomfield et al., 2020a). Such an approach could help to test the sensitivity of compound events to different  
526 power system scenarios (e.g., with different wind power installed capacities).

527 With the anticipated rapid growth of onshore and offshore wind farms, the impact of low wind  
528 conditions on power system risks is likely to increase and become a greater threat alongside cold temperature  
529 conditions. As climate change reduces the frequency of cold events (Seneviratne, 2021), future risks to the  
530 French power system may be more evenly spread throughout the winter season, rather than being concentrated  
531 primarily in January and February as they are currently (RTE, 2023, §6.2.5.3). In addition, changes in  
532 electricity demand patterns are also anticipated. During the summer, increased electricity demand is expected  
533 due to higher use of air conditioning in France. However, the risks to the French power system during summer  
534 are expected to be limited thanks to higher solar power production and power system flexibilities (RTE, 2023,  
535 §6.2.5.3). How the risks to the adequacy between electricity generation and demand associated with compound  
536 events will evolve in the next few decades is therefore multifaceted, depending on future levels of installed  
537 wind power capacity, changes in demand patterns, and climate change. We plan to address some of these  
538 questions in future work using climate projections from the latest Coupled Model Intercomparison Project  
539 Phase 6.

540 Future risks to the electricity system will also depend on the amount of electricity that can be stored to  
541 modulate the variability of renewable energy production. In this context, long-lasting compound low wind  
542 and cold events at the European scale will be of particular relevance. The study of such long events impacting  
543 a large domain requires a large sample. The use of the ERA5 reanalysis in this context is therefore not  
544 appropriate. An interesting option is to use state of the art Earth System Models, which provide large

545 ensembles of simulations that enable identifying a higher number of long and high impact compound events  
546 (Bevacqua et al., 2023).

547 How the occurrence of compound events will continue to evolve in a changing climate is also a crucial  
548 question in the context of the energy transition. This study lays a methodological groundwork for addressing  
549 this question. It can also serve as a reference for the evaluation and selection of climate models that could then  
550 be used to assess the projections in compound events. In particular, our findings highlight the important role  
551 of the large-scale atmospheric circulation in driving compound low wind and cold events in winter in France,  
552 and this contribution is therefore a relevant metric for model evaluation in this context.  
553

## 554 **Statements & Declarations**

555 **Fundings.** This study is part of a PhD project funded by Réseau de Transport d'Electricité (RTE).

556 **Competing Interests.** The authors declare they have no conflict of interest.

557 **Author contributions.** All authors contributed to the conception and design of the study. Data collection and  
558 analysis were performed by FC, MB and JB. All authors contributed to the interpretation of the results. The  
559 first draft of the manuscript was written by FC, MB and JB and all authors commented on previous versions  
560 of the manuscript. All authors read and approved the final manuscript.

561 **Data availability.** The ERA5 reanalysis data are available on the Copernicus Data Store (CDS) at  
562 <https://cds.climate.copernicus.eu/cdsapp#!/dataset/reanalysis-era5-single-levels?tab=overview> (Hersbach et  
563 al., 2020). The MERRA-2 reanalysis data are available from NASA at  
564 [https://disc.gsfc.nasa.gov/datasets/M2T1NXLND\\_5.12.4/summary](https://disc.gsfc.nasa.gov/datasets/M2T1NXLND_5.12.4/summary) (Gelaro et al., 2017). The E-OBS gridded  
565 in situ observation datasets are provided by the European Climate Assessment & Dataset and available at:  
566 <https://www.ecad.eu/download/ensembles/download.php>.

567

568

- 570 Añel, J., Fernández-González, M., Labandeira, X., López-Otero, X., and De La Torre, L.: Impact of Cold  
571 Waves and Heat Waves on the Energy Production Sector, *Atmosphere*, 8, 209,  
572 <https://doi.org/10.3390/atmos8110209>, 2017.
- 573  
574 Bevacqua, E., Suarez-Gutierrez, L., Jézéquel, A., Lehner, F., Vrac, M., Yiou, P., and Zscheischler, J.:  
575 Advancing research on compound weather and climate events via large ensemble model simulations, *Nat*  
576 *Commun*, 14, 2145, <https://doi.org/10.1038/s41467-023-37847-5>, 2023.
- 577  
578 Bloomfield, H. C., Brayshaw, D. J., and Charlton-Perez, A. J.: Characterizing the winter meteorological  
579 drivers of the European electricity system using targeted circulation types, *Meteorol Appl*, 27,  
580 <https://doi.org/10.1002/met.1858>, 2020a.
- 581  
582 Bloomfield, H. C., Brayshaw, D. J., Deakin, M., and Greenwood, D.: Hourly historical and near-future weather  
583 and climate variables for energy system modelling, *Earth Syst. Sci. Data*, 14, 2749–2766,  
584 <https://doi.org/10.5194/essd-14-2749-2022>, 2022.
- 585  
586 Boé, J., Mass, A., and Deman, J.: A simple hybrid statistical–dynamical downscaling method for emulating  
587 regional climate models over Western Europe. Evaluation, application, and role of added value?, *Clim Dyn*,  
588 61, 271–294, <https://doi.org/10.1007/s00382-022-06552-2>, 2023.
- 589  
590 Cassou, C.: Intraseasonal interaction between the Madden–Julian Oscillation and the North Atlantic  
591 Oscillation, *Nature*, 455, 523–527, <https://doi.org/10.1038/nature07286>, 2008.
- 592  
593 Cattiaux, J., Vautard, R., Cassou, C., Yiou, P., Masson-Delmotte, V., and Codron, F.: Winter 2010 in Europe:  
594 A cold extreme in a warming climate, *Geophysical Research Letters*, 37, 2010GL044613,  
595 <https://doi.org/10.1029/2010GL044613>, 2010.
- 596  
597 Cornes, R. C., Van Der Schrier, G., Van Den Besselaar, E. J. M., and Jones, P. D.: An Ensemble Version of  
598 the E-OBS Temperature and Precipitation Data Sets, *JGR Atmospheres*, 123, 9391–9409,  
599 <https://doi.org/10.1029/2017JD028200>, 2018.
- 600  
601 Deser, C. and Phillips, A. S.: A range of outcomes: the combined effects of internal variability and  
602 anthropogenic forcing on regional climate trends over Europe, *Nonlin. Processes Geophys.*, 30, 63–84,  
603 <https://doi.org/10.5194/npg-30-63-2023>, 2023.
- 604  
605 Deser, C., Terray, L., and Phillips, A. S.: Forced and Internal Components of Winter Air Temperature Trends  
606 over North America during the past 50 Years: Mechanisms and Implications\*, *Journal of Climate*, 29, 2237–  
607 2258, <https://doi.org/10.1175/JCLI-D-15-0304.1>, 2016.
- 608  
609 Falkena, S. K. J., de Wiljes, J., Weisheimer, A., and Shepherd, T. G.: Revisiting the Identification of  
610 Wintertime Atmospheric Circulation Regimes in the Euro-Atlantic Sector, *Quart J Royal Meteorol Soc*, 146,  
611 2801–2814, <https://doi.org/10.1002/qj.3818>, 2020.
- 612  
613 Gelaro, R., McCarty, W., Suárez, M. J., Todling, R., Molod, A., Takacs, L., Randles, C. A., Darmenov, A.,  
614 Bosilovich, M. G., Reichle, R., Wargan, K., Coy, L., Cullather, R., Draper, C., Akella, S., Buchard, V., Conaty,  
615 A., Da Silva, A. M., Gu, W., Kim, G.-K., Koster, R., Lucchesi, R., Merkova, D., Nielsen, J. E., Partyka, G.,  
616 Pawson, S., Putman, W., Rienecker, M., Schubert, S. D., Sienkiewicz, M., and Zhao, B.: The Modern-Era  
617 Retrospective Analysis for Research and Applications, Version 2 (MERRA-2), *J. Climate*, 30, 5419–5454,  
618 <https://doi.org/10.1175/JCLI-D-16-0758.1>, 2017.
- 619  
620 Grams, C. M., Beerli, R., Pfenninger, S., Staffell, I., and Wernli, H.: Balancing Europe’s wind-power output  
621 through spatial deployment informed by weather regimes, *Nature Clim Change*, 7, 557–562,

622 <https://doi.org/10.1038/nclimate3338>, 2017.

623

624 Hersbach, H., Bell, B., Berrisford, P., Hirahara, S., Horányi, A., Muñoz-Sabater, J., Nicolas, J., Peubey, C.,  
625 Radu, R., Schepers, D., Simmons, A., Soci, C., Abdalla, S., Abellan, X., Balsamo, G., Bechtold, P., Biavati,  
626 G., Bidlot, J., Bonavita, M., Chiara, G., Dahlgren, P., Dee, D., Diamantakis, M., Dragani, R., Flemming, J.,  
627 Forbes, R., Fuentes, M., Geer, A., Haimberger, L., Healy, S., Hogan, R. J., Hólm, E., Janisková, M., Keeley,  
628 S., Laloyaux, P., Lopez, P., Lupu, C., Radnoti, G., Rosnay, P., Rozum, I., Vamborg, F., Villaume, S., and  
629 Thépaut, J.: The ERA5 global reanalysis, *Q.J.R. Meteorol. Soc.*, 146, 1999–2049,  
630 <https://doi.org/10.1002/qj.3803>, 2020.

631

632 Hirschi, J. J. -M. and Sinha, B.: Negative NAO and cold Eurasian winters: how exceptional was the winter of  
633 1962/1963?, *Weather*, 62, 43–48, <https://doi.org/10.1002/wea.34>, 2007.

634

635 Horton, D. E., Johnson, N. C., Singh, D., Swain, D. L., Rajaratnam, B., and Diffenbaugh, N. S.: Contribution  
636 of changes in atmospheric circulation patterns to extreme temperature trends, *Nature*, 522, 465–469,  
637 <https://doi.org/10.1038/nature14550>, 2015.

638

639 Jourdier, B.: Evaluation of ERA5, MERRA-2, COSMO-REA6, NEWA and AROME to simulate wind power  
640 production over France, *Adv. Sci. Res.*, 17, 63–77, <https://doi.org/10.5194/asr-17-63-2020>, 2020.

641

642 Lorenz, E. N.: Atmospheric Predictability as Revealed by Naturally Occurring Analogues, *Journal of*  
643 *Atmospheric Sciences*, 26, 636–646, [https://doi.org/10.1175/1520-0469\(1969\)26<636:APARBN>2.0.CO;2](https://doi.org/10.1175/1520-0469(1969)26<636:APARBN>2.0.CO;2),  
644 1969.

645

646 Manwell, J. F.: *Wind Energy Explained: Theory, Design and Application*, n.d.

647

648 Najac, J., Boé, J., and Terray, L.: A multi-model ensemble approach for assessment of climate change impact  
649 on surface winds in France, *Clim Dyn*, 32, 615–634, <https://doi.org/10.1007/s00382-008-0440-4>, 2009.

650

651 Olauson, J.: ERA5: The new champion of wind power modelling?, *Renewable Energy*, 126, 322–331,  
652 <https://doi.org/10.1016/j.renene.2018.03.056>, 2018.

653

654 Otero, N., Martius, O., Allen, S., Bloomfield, H., and Schaeffli, B.: A copula-based assessment of renewable  
655 energy droughts across Europe, *Renewable Energy*, 201, 667–677,  
656 <https://doi.org/10.1016/j.renene.2022.10.091>, 2022a.

657

658 Otero, N., Martius, O., Allen, S., Bloomfield, H., and Schaeffli, B.: Characterizing renewable energy  
659 compound events across Europe using a logistic regression-based approach, *Meteorological Applications*, 29,  
660 <https://doi.org/10.1002/met.2089>, 2022b.

661

662 Plaut, G. and Simonnet, E.: Large-scale circulation classification, weather regimes, and local climate over  
663 France, the Alps and Western Europe, *Clim. Res.*, 17, 303–324, <https://doi.org/10.3354/cr017303>, 2001.

664

665 Rapella, L., Faranda, D., Gaetani, M., Drobinski, P., and Ginesta, M.: Climate change on extreme winds  
666 already affects off-shore wind power availability in Europe, *Environ. Res. Lett.*, 18, 034040,  
667 <https://doi.org/10.1088/1748-9326/acbdb2>, 2023.

668

669 Ravestein, P., Van Der Schrier, G., Haarsma, R., Scheele, R., and Van Den Broek, M.: Vulnerability of  
670 European intermittent renewable energy supply to climate change and climate variability, *Renewable and*  
671 *Sustainable Energy Reviews*, 97, 497–508, <https://doi.org/10.1016/j.rser.2018.08.057>, 2018.

672

673 Raynaud, D., Hingray, B., François, B., and Creutin, J. D.: Energy droughts from variable renewable energy  
674 sources in European climates, *Renewable Energy*, 125, 578–589,  
675 <https://doi.org/10.1016/j.renene.2018.02.130>, 2018.

676 RTE (Réseau de transport d'électricité), *Futurs énergétiques 2050*, octobre 2021.

677 RTE (Réseau de transport d'électricité). Bilan prévisionnel. *Futurs énergétiques 2050. 2023-2035 : première*  
678 *étape vers la neutralité carbone.*

679

680 Saffioti, C., Fischer, E. M., Scherrer, S. C., and Knutti, R.: Reconciling observed and modeled temperature  
681 and precipitation trends over Europe by adjusting for circulation variability, *Geophysical Research Letters*,  
682 43, 8189–8198, <https://doi.org/10.1002/2016GL069802>, 2016.

683

684 Seneviratne, S.I., X. Zhang, M. Adnan, W. Badi, C. Dereczynski, A. Di Luca, S. Ghosh, I. Iskandar, J. Kossin,  
685 S. Lewis, F. Otto, I. Pinto, M. Satoh, S.M. Vicente-Serrano, M. Wehner, and B. Zhou: *Weather and Climate*  
686 *Extreme Events in a Changing Climate.*, 1st ed., Cambridge University Press,  
687 <https://doi.org/10.1017/9781009157896>, 2021.

688

689 Shepherd, T. G.: Atmospheric circulation as a source of uncertainty in climate change projections, *Nature*  
690 *Geosci*, 7, 703–708, <https://doi.org/10.1038/ngeo2253>, 2014.

691

692 Sippel, S., Meinshausen, N., Merrifield, A., Lehner, F., Pendergrass, A. G., Fischer, E., and Knutti, R.:  
693 Uncovering the Forced Climate Response from a Single Ensemble Member Using Statistical Learning, *Journal*  
694 *of Climate*, 32, 5677–5699, <https://doi.org/10.1175/JCLI-D-18-0882.1>, 2019.

695

696 Sippel, S., Fischer, E. M., Scherrer, S. C., Meinshausen, N., and Knutti, R.: Late 1980s abrupt cold season  
697 temperature change in Europe consistent with circulation variability and long-term warming, *Environ. Res.*  
698 *Lett.*, 15, 094056, <https://doi.org/10.1088/1748-9326/ab86f2>, 2020.

699

700 Staffell, I. and Pfenninger, S.: Using bias-corrected reanalysis to simulate current and future wind power  
701 output, *Energy*, 114, 1224–1239, <https://doi.org/10.1016/j.energy.2016.08.068>, 2016.

702

703 Tedesco, P., Lenkoski, A., Bloomfield, H. C., and Sillmann, J.: Gaussian copula modeling of extreme cold  
704 and weak-wind events over Europe conditioned on winter weather regimes, *Environ. Res. Lett.*, 18, 034008,  
705 <https://doi.org/10.1088/1748-9326/acb6aa>, 2023.

706

707 Terray, L.: A dynamical adjustment perspective on extreme event attribution, *Weather Clim. Dynam.*, 2, 971–  
708 989, <https://doi.org/10.5194/wcd-2-971-2021>, 2021.

709

710 Thornton, H. E., Scaife, A. A., Hoskins, B. J., and Brayshaw, D. J.: The relationship between wind power,  
711 electricity demand and winter weather patterns in Great Britain, *Environ. Res. Lett.*, 12, 064017,  
712 <https://doi.org/10.1088/1748-9326/aa69c6>, 2017.

713

714 Van Den Dool, H. M.: Searching for analogues, how long must we wait?, *Tellus A*, 46, 314–324,  
715 <https://doi.org/10.1034/j.1600-0870.1994.t01-2-00006.x>, 1994.

716

717 Van Oldenborgh, G. J., Mitchell-Larson, E., Vecchi, G. A., De Vries, H., Vautard, R., and Otto, F.: Cold  
718 waves are getting milder in the northern midlatitudes, *Environ. Res. Lett.*, 14, 114004,  
719 <https://doi.org/10.1088/1748-9326/ab4867>, 2019.

720

721 van der Wiel, K., Stoop, L. P., van Zuijlen, B. R. H., Blackport, R., van den Broek, M. A., and Selten, F. M.:  
722 Meteorological conditions leading to extreme low variable renewable energy production and extreme high  
723 energy shortfall, *Renewable and Sustainable Energy Reviews*, 111, 261–275,  
724 <https://doi.org/10.1016/j.rser.2019.04.065>, 2019a.

725

726 van der Wiel, K., Bloomfield, H. C., Lee, R. W., Stoop, L. P., Blackport, R., Screen, J. A., and Selten, F. M.:  
727 The influence of weather regimes on European renewable energy production and demand, *Environ. Res. Lett.*,  
728 14, 094010, <https://doi.org/10.1088/1748-9326/ab38d3>, 2019b.

729  
730  
731  
732  
733  
734  
735

Zscheischler, J., Martius, O., Westra, S., Bevacqua, E., Raymond, C., Horton, R. M., van den Hurk, B., AghaKouchak, A., Jézéquel, A., Mahecha, M. D., Maraun, D., Ramos, A. M., Ridder, N. N., Thiery, W., and Vignotto, E.: A typology of compound weather and climate events, *Nat Rev Earth Environ*, 1, 333–347, <https://doi.org/10.1038/s43017-020-0060-z>, 2020.